MIT Open Access Articles

Toward directed energy planetary defense

Toward directed energy planetary defense

Philip Lubin
Gary B. Hughes
Johanna Bible
Jesse Bublitz
Josh Arriola
Caio Motta
Jon Suen
Isabella Johansson
Jordan Riley
Nilou Sarvian
Deborah Clayton-Warwick
Jane Wu
Andrew Milich
Mitch Oleson
Mark Pryor
Peter Krogen
Miikka Kangas
Hugh O'Neill

Toward directed energy planetary defense

Philip Lubin,[a,*] Gary B. Hughes,[b] Johanna Bible,[a] Jesse Bublitz,[a] Josh Arriola,[a] Caio Motta,[a] Jon Suen,[a] Isabella Johansson,[a] Jordan Riley,[a] Nilou Sarvian,[a] Deborah Clayton-Warwick,[a] Jane Wu,[a] Andrew Milich,[a] Mitch Oleson,[a] Mark Pryor,[c] Peter Krogen,[d] Miikka Kangas,[a] and Hugh O'Neill[e]

[a]University of California, Physics Department, Santa Barbara, California 93106-9530
[b]California Polytechnic State University, Statistics Department, San Luis Obispo, California 93407-0405
[c]Vorticy Inc., San Diego, California 92121
[d]MIT, Electrical Engineering and Computer Science, Cambridge, Massachusetts 02139-4307
[e]California Polytechnic State University, Physics Department, San Luis Obispo, California 93407-0405

Abstract. Asteroids and comets that cross Earth's orbit pose a credible risk of impact, with potentially severe disturbances to Earth and society. We propose an orbital planetary defense system capable of heating the surface of potentially hazardous objects to the vaporization point as a feasible approach to impact risk mitigation. We call the system DE-STAR, for Directed Energy System for Targeting of Asteroids and exploRation. The DE-STAR is a modular-phased array of kilowatt class lasers powered by photovoltaic's. Modular design allows for incremental development, minimizing risk, and allowing for technological codevelopment. An orbiting structure would be developed in stages. The main objective of the DE-STAR is to use focused directed energy to raise the surface spot temperature to ~3000 K, sufficient to vaporize all known substances. Ejection of evaporated material creates a large reaction force that would alter an asteroid's orbit. The baseline system is a DE-STAR 3 or 4 (1- to 10-km array) depending on the degree of protection desired. A DE-STAR 4 allows initial engagement beyond 1 AU with a spot temperature sufficient to completely evaporate up to 500-m diameter asteroids in 1 year. Small objects can be diverted with a DE-STAR 2 (100 m) while space debris is vaporized with a DE-STAR 1 (10 m). © *2014 Society of Photo-Optical Instrumentation Engineers (SPIE)* [DOI: 10.1117/1.OE.53.2.025103]

Keywords: asteroid impact; directed energy; laser-phased array; planetary defense.

Paper 131426P received Sep. 14, 2013; revised manuscript received Dec. 31, 2013; accepted for publication Jan. 6, 2014; published online Feb. 18, 2014.

1 Introduction

Recent advances in photonics make a scientific discussion of directed energy planetary defense feasible whereas even 10 years ago it was close to science fiction. High-power lasers are capable of delivering sufficient energy density on a target to melt and vaporize any known material. Laser machining and welding are commonplace in industry, where even refractory metals are directly machined or joined with lasers. Scaling of laser technology has spurred development of directed energy systems that are capable of delivering high energy density on distant targets. Recent developments have resulted in conversion of electrical to photon efficiencies of close to 50% with powers in excess of 1 kW per (handheld) unit. Additionally, and critical for this program, such devices can be phased locked. This field is rapidly changing and even more efficient devices with higher power density will be available in the near future. This allows us to contemplate directed energy systems for large-scale deployment. Inside the Earth's atmosphere, the directed energy systems are hindered by atmospheric fluctuations of the coherent beam. A directed energy system deployed above the atmosphere could project a beam through space unfettered by atmospheric interference and thus allows us to design systems that are essentially diffraction limited as the interplanetary medium is extremely tenuous and does not affect the laser beam significantly. This paper describes a feasible design for a future orbiting standoff-directed energy system, which we call DE-STAR for Directed Energy System for Targeting of Asteroids and exploRation. The system consists of an array of phase-locked modest power laser amplifiers. By controlling the relative phases of individual laser elements, the combined beam can be directed to a distant target. Lasers are powered by solar photovoltaics of essentially the same area as the laser array. By increasing the array size, we can both reduce the spot size due to diffraction and increase the power. This dual effect allows us to vaporize elements on the surface of asteroids at distances that are significant compared to the solar system. By raising the flux (W/m^2) on the target asteroid to a sufficiently high level, we can begin direct evaporation of the asteroid at the spot. This has two basic effects. First, we directly begin to evaporate the asteroid and given sufficient time, a threatening asteroid could be totally vaporized before hitting the Earth. Second, evaporation at the spot causes a back reaction on the asteroid from the vaporization plume, which acts as a rocket and thus the asteroid can be deflected. This paper explores the potential capabilities of the system for mitigating the threat of asteroid impact. Since the DE-STAR is a phased array consisting of a very large number of elements, it can simultaneously be used for multiple purposes and is intrinsically a multitasking system. Figure 1 depicts an orbiting DE-STAR system simultaneously engaged in both evaporating and deflecting a large asteroid as well as powering and propelling a spacecraft. As this is a modular system, we classify each DE-STAR by the log of its linear size, thus, a DE-STAR 1 is 10 m, DE-STAR 2 is 100 m etc. A DE-STAR 4 system will produce a reaction thrust comparable to the shuttle solid rocket booster (SRB)

on the asteroid due to mass ejection and thus allow for orbital diversion of even larger asteroids, beyond several kilometers in diameter, thus allowing for protection from every known asteroid threat. Smaller systems are also extremely useful. For example, a DE-STAR 2 (100-m array) would be capable of diverting volatile-laden objects 100 m in diameter by initiating engagement at ∼0.01 to 0.5 AU (AU = astronomical unit = mean distance from Earth to Sun ∼ 1.5×10^{11} m). Smaller objects could be diverted on shorter notice. The phased array configuration is capable of creating multiple beams, so a single DE-STAR of sufficient size could engage several threats simultaneously, such as a Shoemaker-Levy 9 scenario on Earth. An orbiting DE-STAR would also be capable a wide variety of other functions. Narrow bandwidth and precision beam control would aid narrow search and ephemeris refinement of objects identified with wide-field surveys. Propulsion of kinetic or nuclear-tipped asteroid interceptors or other interplanetary spacecraft is possible using the "photon rail gun" mode from direct photon pressure on a spacecraft, propelling a 100-kg craft to 1 AU in 3 days and a 10,000-kg craft to 1 AU in 30 days. A DE-STAR could also provide power to ion propulsion systems, providing both a means of acceleration on the outbound leg, and deceleration for orbit. Ideally, two systems would provide the ability to "ping pong" spacecraft if this were needed, though this is vastly more challenging. Vaporization and de-orbiting of debris in Earth orbit could be accomplished with a DE-STAR 1 or 2 system. The DE-STAR 3 and 4 arrays may allow stand-off interrogation of asteroid composition by observing absorption lines in the blackbody spectrum of a vaporizing surface spot. There are a number of other applications as well, including downlink power via millimeter, microwave, or laser—the so-called space power system or space power satellite (SPS) mode. The system is a standoff planetary defense system that is always ready when needed and no dedicated mission is needed for each threat as is the case with other proposed mitigation methods.

The multipurpose aspect of the system allows it to be useful with very high "duty cycle." The DE-STAR system is inherently modular and scalable thus allowing us to build and test smaller units both in the lab, on the ground and in suborbital test flights on balloons. Each module is modest in size and power and identical allowing for mass production. This is key to cost reduction. Each element uses only modest laser power and thus the areal power density is low (<1 kW/m^2). It is inherently redundant since each module is largely self contained and thus failure of modest numbers of elements has little effect. The flux on target (W/m^2) at a fixed distance scales as the d^4 where d is the linear dimension of the array and thus it increases very rapidly with increased size. This system is useful for many other purposes, which are briefly mentioned in this article (and discussed in greater detail in other SPIE Optics & Photonics 2013 Proceedings papers, including Hughes et al.[1] and Bible et al.[2]).

2 Laser-Phased Arrays

2.1 System Architecture

Planar arrays of phase-locked lasers have been developed in the laboratory. Vorontsov et al.[3] describe a phased array of densely packed fiber laser collimators. The system utilizes adaptive dynamic phase distortion compensation to accomplish phase locking across the laser array. Other schemes for combining coherent beams have also been described.[4] The efficiency of laser fiber amplifiers has undergone a remarkable revolution in the last decade resulting from both the telecom industry and the commercial need for high-power solid-state lasers for machining, among other tasks. With efficiencies already close to 50% for the lasers and with solar cells near 50% efficient we can realistically consider such a system. Our basic approach is to use existing technology without requiring any "miracles" but with reasonable expectations for modest improvements, with an eye toward new devices that may be superior, but the basic fact remains—it is now possible with high efficiency to convert light from the sun into a highly focused coherent beam capable of planetary-scale defense. We feel it is now inevitable that this will be done and rapid progress with modest costs can begin this process that will lead to a full defensive capability. With efficiencies approaching unity, we only project modest improvements (factor of 2) in efficiency but see a rapid improvement in power density (kW/kg). Although current power density is about 0.2 kW/kg using Ytterbium (Yb)-doped fiber amplifiers, a relatively rapid roadmap to 1 kW/kg is already in place. In the next decade, we expect an order of magnitude increase in this. The current DARPA Excalibur program is one example of pursuing high-efficiency fiber fed lasers. Excalibur goals are multikilowatt fiber 1.06-μm wavelength laser amplifiers with a target of >0.2 kW/kg with near 40% efficiency for the laser amplifier. Efficiency goals are comparable to current light-emitting diodes (LEDs) that are already about 50% efficient. Coincidentally, on the space photovoltaic (PV) side, the power density is nearly identical at 0.1 kW/kg (UltraFlex, from ATK, Goleta, California) with modest term possibilities for increasing this to 1 kW/kg. Recent work on inverted metamorphic multijunction cells promises >0.5 kW/kg. Another option would be to beam power (via mm or microwave) from the ground to the system so no PV is needed. This would be most natural for a geo-sync orbit which requires significantly more launch capability or a laser boot strap LEO to GEO approach. Maintenance in such a case is much more difficult and the rectenna mass would have to be compared to the PV mass.

Long coherence length is critical and the existing fiber-based laser amplifiers are already good enough (depending on the mode they are operated in), though new advances are becoming available to allow the stimulated Brillouin scattering (SBS) limit to be extended with even longer coherence lengths. With the current technology a DE-STAR 2 program could be started, leading to launch and possibly a DE-STAR 3. We advocate a conservative and logical approach of rapidly building smaller and much lower cost units (DE-STAR 0 and 1), testing on the ground, and then as technology catches up and technological and system problems arise and are solved and move to larger systems, eventually leading to orbital testing and scale up to the full defensive goal. The system is not binary in that small systems have immediate applications (DE-STAR 1 space debris for example) as larger systems are being developed for comet and small asteroid protection (DE-STAR 2) leading eventually to a DE-STAR 3 or 4.

As a goal, we studied the feasibility of a system possessing the capability to evaporate, prior to impact, asteroids in

the size range 150 m to 1 km, and with typical orbital closing speeds. These stated capabilities drive system requirements into the multikilometers class array size for both the diffraction limit of the optics and the power required. As a specific example, we could seek to evaporate an Apophis-class asteroid (325-m diameter) with a worst case assumption of complete chemical binding and <1 year to evaporate the entire boloid, with a desired interdiction starting at 1 AU. A 10-km DE-STAR system would be capable of meeting the stated goal as shown in the calculations presented below. It is also fortuitous that the same size system required to form a small spot on the distant asteroid from the diffraction limit, assuming a wavelength near 1 μm, is also about the same size as needed to power the laser amplifiers in order to raise the flux to the evaporation point from converting sunlight that falls on the DE-STAR into electricity. At the Earth's orbit the "solar constant" is about 1400 W/m^2 or 1.4 (140) GW of sunlight on a 1 (10)-km-sized solar array. This is sufficient to power the entire system and no additional power is needed. This also forms a very large potential for an SPS system to send excess power to the Earth. By utilizing a filled array of solar-powered phase-locked lasers, there is a near ideal convergence of size required to both power the system and to produce the diffraction-limited beam needed to begin vaporization. Baseline calculations are developed using a 1.06-μm wavelength, to produce sufficient flux at 1 AU that will sustain evaporation, which requires greater than $\sim$5-MW/m^2 flux at target. As stated existing Yb laser fiber amplifiers at 1.06-μm wavelength have efficiencies near 40%. Space solar PV has efficiency of about 35% in one sun (not concentrated) with near 50% when concentrated. We assume modest efficiency improvements of both laser and PV to 70%, which is not unreasonable in the realistic time scale of a full DE-STAR

4 system. We thus assume overall conversion efficiency of sunlight to laser power of about 50%, resulting in $\sim$0.7 GW/km^2 of laser power. Even with current efficiencies and no improvements the system would work well today, though with ($\sim$3$\times$) lower evaporation rates which does not change the basic conclusions. Increases in efficiency however are inevitable. For a 1-km system laser power would be 0.7 GW whereas a 10-km system would have laser power of 70 GW, which is more than sufficient for meeting the stated goal of surface vaporization at 1 AU of all known materials. One major advantage of a phased array is that multiple independent beams can be produced, so multiple targets or efforts can be simultaneously engaged. For reference, we note that 70 GW is the equivalent of about 1.4 MT (megatons TNT—1 MT $\sim 4.2 \times 10^{15}$ J) per day or about 500 MT per year of potentially deliverable energy, a significant portion of the total currently active US nuclear arsenal. Note that in the process, we also have 100 GW of electrical energy produced or the equivalent of about 100 large utility nuclear reactors. This would allow a very large SPS if needed.

For DE-STAR, launch mass is critical in the costing analysis, so while the required efficiency is already effectively available, the power mass density is where we need to increase significantly. Solar PV cells can be extremely thin, and low areal mass through focusing with thin-film mirrors on solar PV may allow the lowest densities. For example, if 10-μm-thick PV could be produced (this is more of a mechanical issue as thinner films already exist on plastic) a 10^4-m PV array would have a mass of about 3×10^6 kg. The current issue for many space solar cells is the charged particle degradation, which is currently met with a "cover glass" on each side of about 100 μm. If we could meet a laser power density of 10 kW/kg (50$\times$ higher than current)
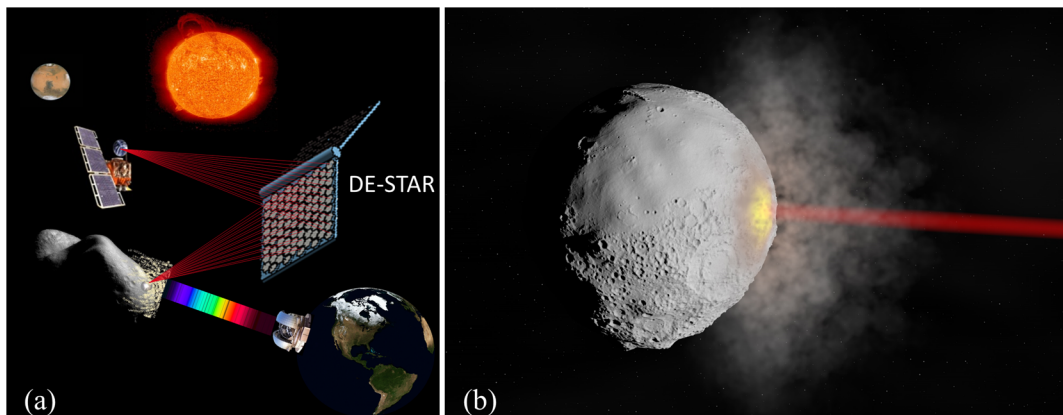

Fig. 1 (a) Concept diagram of an orbiting directed energy system for targeting of asteroids and exploration (DE-STAR) engaged in multiple tasks including asteroid diversion, composition analysis, and long range spacecraft power and propulsion. The system consists of an array of phase-locked lasers. By controlling the relative phases of individual laser elements, the combined beam can be directed to a distant target. Lasers are powered by a solar panel of effectively the same area as the laser array. A DE-STAR of sufficient size would be capable of vaporizing elements on the surface of asteroids. Given sufficient time, a threatening asteroid could be vaporized, deflected or disintegrated prior to impacting Earth. The ability to direct energy onto a distant target renders DE-STAR capable of many functions. Asteroid interrogation may be possible by viewing absorption lines as the heated spot is viewed through the ejected vapor plume. Photon pressure can be used to accelerate (and decelerate) interplanetary spacecraft, among many other possibilities. (b) Visualization with relevant physical phenomenon included at a flux of about 10 MW/m^2. Compare this to the picture of the laboratory test in Fig. 13 where the bright high temperature spot is also visible with about the same flux. The plume density is exaggerated to show ejecta. Asteroid diameter is about that of apophis (325 m) relative to the laser beam diameter (30 m). Target is at 1 AU.

then 70 GW of fiber lasers would be 7×10^6 kg. This mass does not represent the entire DE-STAR system, but the scale is not outrageous. The 10 kW/kg for laser mass density over 20 years is a goal but even the existing 0.2-kW/kg density allows up to nearly a DE-STAR 3 using existing launcher capability. For reference, the International Space Station (ISS) mass is about 0.5×10^6 kg with much more than this being lifted into orbit, as much of it was also returned in shuttle missions. Conservatively, we could thus say we already know how to launch few $\times 10^6$-kg class space missions as we already did so with the ISS. Either heavy lift chemical launchers would be needed to loft DE-STAR 4 modules, or a bootstrap ground-based DE-STAR driven hybrid booster would be required. The modules are being designed around the existing heavy lift fairing size allowing for a 3- to 4-m-diameter class module. The modules can be quite thin and stacked during launch and assembled in orbit. Since the system is a phased array the structure does not need the structural integrity of a conventional mirror but rather must be stiff enough to have vibration modes that are below the metrology servo loop bandwidth as phase control is not handled by keeping the structure stiff but rather by measuring the relative position of each element adjusting the phase shifter in each amplifier to keep the beam on the target. Figure 2 shows system configuration diagram with laser fiber amplifiers. Figure 3 illustrates achievable power at various distances with different array sizes, and the equivalent amount of vaporization that is possible.

2.1.1 Thermal dissipation

The average thermal load (to dissipate) of the system (independent of size) is about 500 W/m^2, which is approximately that of a person (or the Earth). It is equivalent to a 300-K blackbody. The average thermal load is extremely low. The average laser power is also quite low, being about 700 W/m^2, which is less than the solar "constant" on the surface of the Earth which is about 1000 W/m^2. You could literally walk in front of the system when operational and not be harmed (laser glasses are recommended, however).

2.1.2 Optical design

The optical design of a phased array is different than that of a classic optical telescope in that the phasing to achieve
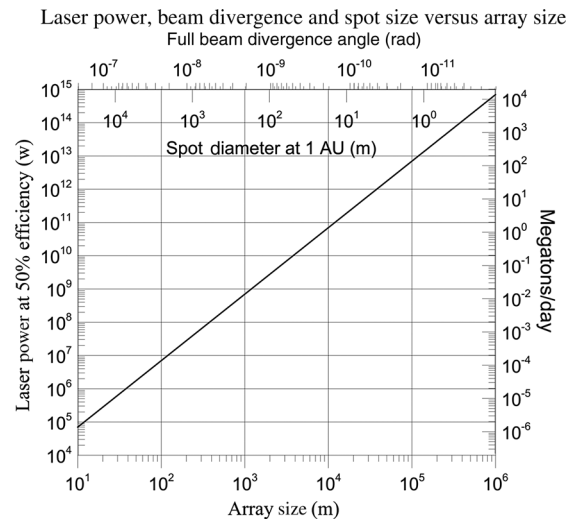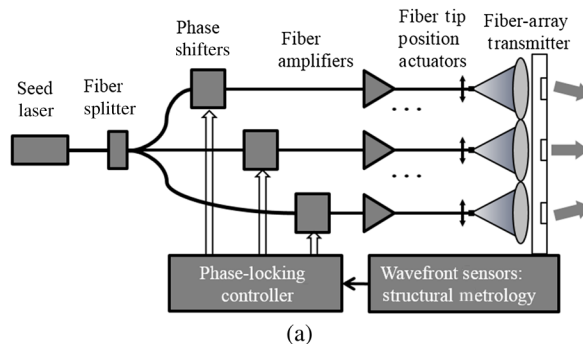

Fig. 3 The DE-STAR laser power, diffraction-limited beam divergence and spot size at target engagement of 1 AU.

constructive interference (which is what allows the image to form) is not done with mechanical alignment as it is in a mirror or lens (where every part of the mirror is essentially a part of the overall "phased array"), but rather the phasing is done by adjusting the phase at each subelement to achieve constructive interference at the target. We are an extremely narrow field of view system and thus we do not have many of the constraints of a classical optical system. We can be any shape for example. We are also extremely narrow bandwidth so thin-film holographic grating diffractive "lenses" become viable. For simplicity, we assume that we will have a roughly planar design with each subelement being either a small reflector or possibly a thin-film holographic lens. The latter has been tried in some narrow-band receiving mode systems and extremely low areal densities have been achieved. This is an area where we need further work to decide on the optimum approach. Our design is a large number of identical low power (700 W/m^2) modules that lend themselves to mass production. Ultralow mass holographic thin-film large-area "lenses" are particularly attractive but SiC- or carbon-fiber-reinforced polymer (CFRP)-replicated reflective optics may be suitable with refinement to lower the mass. In our current baseline, each element has a single fiber amplifier
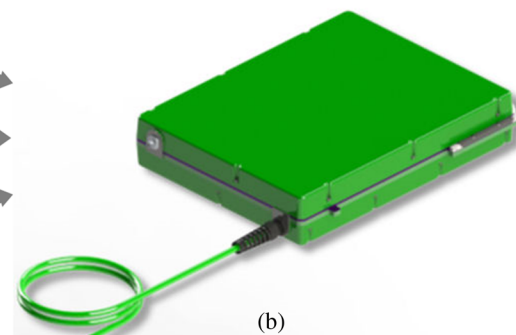
Fig. 2 (a) A system block diagram of the fiber amplifier configuration, based on work by Vorontsov et al.[3] Individual beams combine near the target. Here, coarse beam orientation is accomplished by moving individual fiber amplifier tips in relation to the transmitting element. Fine beam steering and beam combination at the target is accomplished by phase control. (b) Existing 1.5-kW Yb-doped fiber amplifier of the type we baseline. Size is about $30 \times 40 \times 10$ cm. We only need one of these per 2 m^2 of the system.

that feeds an optical element. A single 1-kW amplifier can feed a 1.5-m^2 optic (mirror or lens). Coarse pointing could be accomplished using fiber tip position actuators behind the lens or mirror as appropriate. A fallback option would be to gimbal each element, though this is more complex. Fine pointing is done with electronic phase adjusters at each amplifier input. The phase is also compared at the output and between elements. The metrology of the entire structure becomes a key part of the servo system. There have been a number of orbital programs looking at extremely high-precision laser metrology over long baselines. The most extreme is the laser interferometer space antenna (LISA) gravitational wave detector that set a metric of 20-pm resolution over 5×10^9-m baseline. This is vastly better than we require. We need about 0.1-μm metrology ($\lambda/10$) over 10 km for the full DE-STAR 4. Similarly, the AMD-MOST program has achieved 1-nm resolution over roughly 10-m baselines (limited by the vacuum chamber for testing). At longer wavelengths the Event Horizon telescope has phased locked 1.3-mm wavelength telescopes across the globe (10^7-m baseline) and achieved 0.1-nrad beam formation or the same as our goal. Radio Astron, a Russian and Earth long baseline interferometer, has produced fringes corresponding to 0.04 nrad. Note that since the optical $F\#$ is very large ($\sim 1.5 \times 10^7$ for a DE-STAR—1-AU target) since the asteroid is far away and hence the beam is nearly parallel at the target with a large "depth of focus" $\sim F\#^2 \lambda \sim 2 \times 10^8$ m. The $F\#$ is the ratio of L/d, where L is the target distance and d is the DE-STAR size.

There are a number of challenges to the optical design and the targeting servo system that need to be explored. Asteroids are dynamic, and while motion in angle may be small to us it can still be significant. Typical asteroids move at 10 to 30 km/s, and with a 30-m beam this is 300 to 1000 beam diameters per second in the worst case. The system will be moving in its orbit around Earth, and Earth will be moving

in its orbit around the sun. There are a lot of issues to be worked out. The Hubble Space Telescope (HST) has about a 35-nrad pointing stability over 24 h, as an example. We need better than 0.1-nrad pointing ideally [our beam is 0.2-nrad full-width half-maximum (FWHM) for a DE-STAR 4]. Though, as we show through simulations, we have some latitude in this. Figure 4 depicts results of an optical simulation for a 1000 by 1000 array with 1-m apertures as an example using coherent beam combining.

2.1.3 Coherence length requirements

For a phased array to work properly the light must be coherent over a time and thus length scale sufficient for all elements to be able to interfere. The coherence length required can be calculated by determining the length difference between the various elements with the most extreme case being the conservative limit.

For a planar array of size d and a target of distance L away, the path length difference between the central beam and the outermost beam is $\delta \sim d^2/8L = d/8F\#$ for the case of a target that is normal to the plane of the phased array. As we move off normal the path length difference is $\delta = 1/2d \sin(\theta)$, where θ is the angle of the target off the normal. The worst case is at right angles ($\theta = \pi/2$) where $\delta = d/2$. If there are controllable optical delays lines then these issues are drastically mitigated but it is preferable to have long coherence length so delays lines are needed. For a target at $L = 1$ AU $\sim 1.5 \times 10^{11}$ m and a DE-STAR 4 with $d = 10^4$ m that $F\# \sim 1.5 \times 10^7 \rightarrow \delta \sim 80$ μm corresponding to a coherence time $t_c = \delta/c \sim 0.3$ ps. For the worst case of $\delta = d/2$ the equivalent $t_c = \delta/c \sim 17$ μs. We want the laser coherence time to be greater than these times. The "coherence bandwidth" of the current Yb fiber amplifiers is intrinsically about 5 to 10 kHz (with corresponding coherence times $t_c \sim 100$ μs or comfortably longer than our worst case). For amplifiers run at their highest power level this "coherence
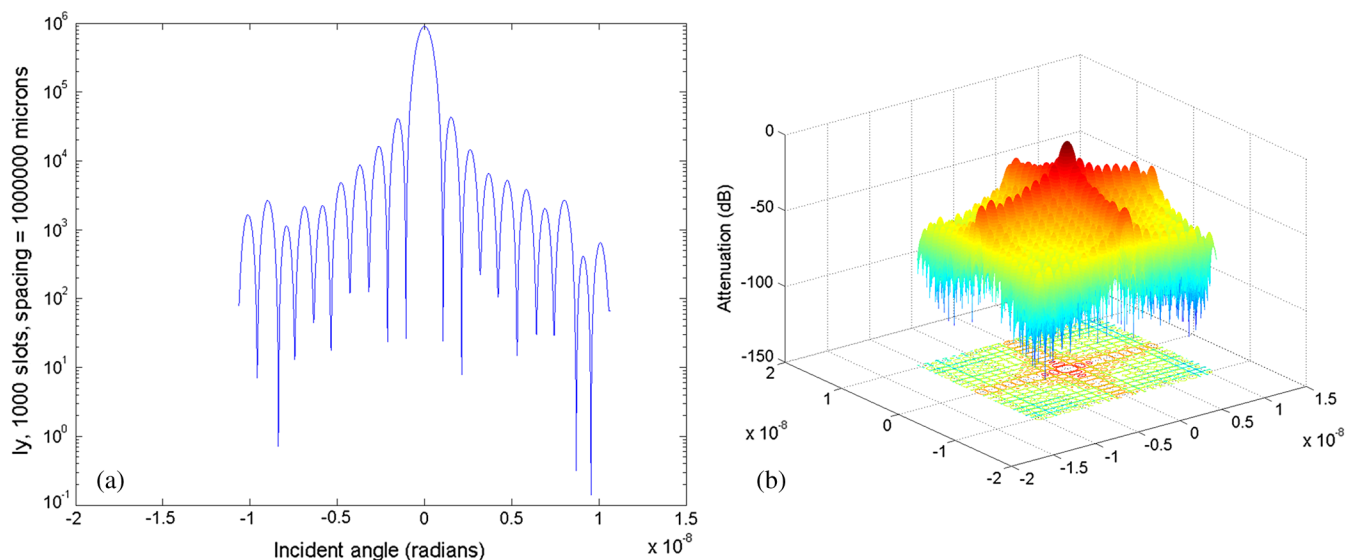
Fig. 4 Simulation results showing coherent beam combining of a 1000 by 1000 element laser array, with 1-m square apertures and close-packed spacing. The simulation included independent-fixed Gaussian-distributed phase shift on every emitter, with 1σ of $\lambda/20$. (a) One-dimensional far-field intensity over a small range of viewing angles. The close-packed array diminishes side lobes and amplifies the central peak. (b) Two-dimensional (2-D) far-field power as attenuation from the maximum intensity in the central lobe.

bandwidth" is generally artificially broadened to about 10 GHz (100 ps) in order to overcome what is known as the SBS limit that limits the amplification power. This is well above the normal incidence case but allows extremely little pointing margin. For example, even a 1-deg pointing difference will give a path length difference of $\delta = 1/2d\sin(\theta) \sim 90$ m with a corresponding coherence time $t_c = \delta/c \sim 300$ ns. When the amplifier is run at a few hundred watts versus kilowatts the "coherence bandwidth" is about 5 to 10 kHz or less as above. The solution to this is to run at normal incidence (not really a good option), add path delay lines (also not a good option in general) or run the amplifiers well outside the SBS limit where the coherence time is longer. The latter is the preferred option. There is technology that has been developed that appears to allow the Yb amplifiers to run at both relatively high power and with long coherence time. This is one of the development items on the roadmap. Since volume (as opposed to mass) is not as much of an issue there may be a trade space that we can exploit to allow for better performance. Note that the deviation of the planar array from a sphere with radius $R = L$ is $\xi = d^2/8R = d^2/8L \sim 80$ μm and deviation of the array plane from a classic optic with focal length $f = L$ is $\xi = d^2/16f = d^2/16L \sim 40$ μm. The array is indeed quite planar!

2.1.4 Space qualification issues

The DE-STAR system is a complex system of both power conversion (solar to electrical to laser) and metrology and targeting among many others. Solar PV is a mature technology and the space qualification and "rad hardening" issues are understood. The situation for fiber amplifiers needs to be addressed as a part of the roadmap. Much of this can be done on the ground in accelerator beam lines and some early long term space exposure will help with determining what issues, if any, are critical to address in this area. The long term exposure to radiation is not well understood for fiber amplifiers and needs to be addressed. Rad hardening of thin film holographic lenses (if we go this route) also needs to be addressed as does lowering the areal mass of space PV, which is often dominated by the glass used to reduce charged particle (mostly electron) damage.

2.2 System Requirements to Evaporate Asteroids

We can calculate the energy required to melt and vaporize the various materials that are common in S-Type (Si rich), C-Type (carbon rich), and M-Type (metal rich) asteroids. Comets are much easier to vaporize in that they do not require a high temperature to begin significant mass ejection. The gravitation binding energy of a molecule to a typical asteroid is very small and is negligible compared to the chemical binding energy. The chemical bonding energy that requires us to heat the spot to high temperature can be expressed through the heat of vaporization. The heat of fusion (melting) is a small fraction of the heat of vaporization. We have modeled the thermal interaction between the laser and asteroid in three ways. The first is a simple analysis based on power only with a flux equivalent to about a 6000-K blackbody. The second method uses detailed calculations of the vapor pressure versus temperature for every element and many of the estimated compounds that are thought to make up asteroids. This is a quasi two-dimensional (2-D) analysis in that it includes radiation emission and mass ejection but ignores thermal conduction. The third method uses all the calculations from the second method but uses a full three-dimensional (3-D) finite element analysis (FEA) of spherical (we can do any shape) asteroids with various thermal conductivities. All three methods give essentially the same answers but we wanted to confirm our calculations with increasingly sophisticated simulations. The final method is a laboratory test system that uses a 19 element laser array to produce a spot flux similar to that of the full DE-STAR 4 at 1 AU, namely about 40 MW/m^2 and targets "rock" samples with similar compositions to asteroids. This testing has begun and will continue over the next year to cross check our simulations for evaporation rates, mass ejection densities, and plume thrusts among other parameters. As expected, when we exceed about 2 MW/m^2 most materials begin to significantly vaporize.

The energy required to melt an asteroid is given by the heat of fusion and required increase in temperature to bring it to the melting point from (assumed) initial low temperature starting point. In practice, this is small compared to the heat of fusion and heat of vaporization. The typical energy per m^3 is of order 10^{10} J to vaporize most materials.
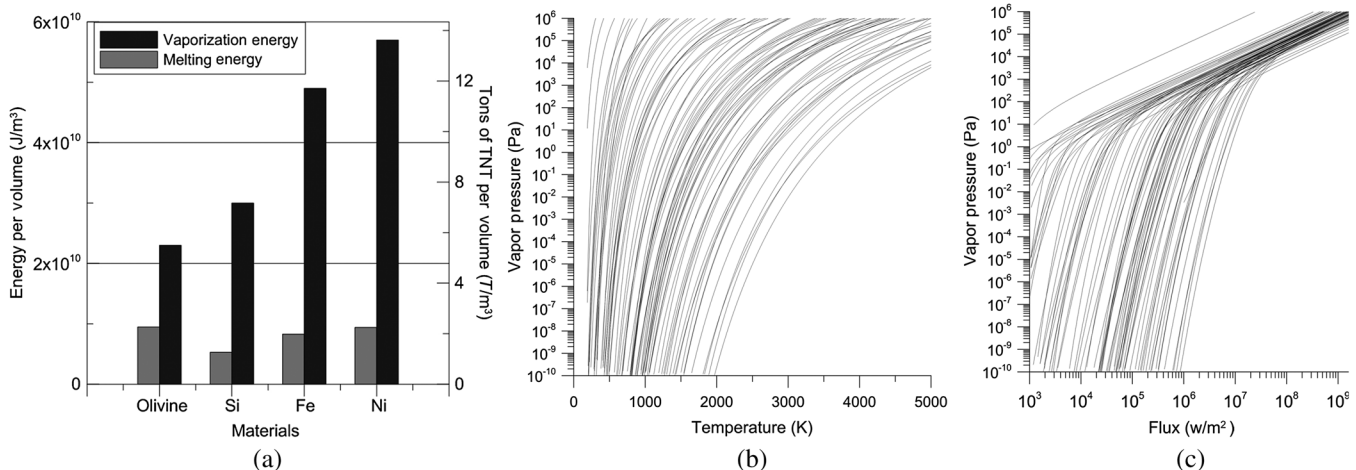

Fig. 5 (a) Melting and vaporization energy per unit volume for S type (Si rich) asteroids. (b) Vapor pressure versus T for virtually all elements on the periodic table (93 are modeled). (c) Vapor pressure versus target flux for the same 93 elements. The upper outlier is mercury.
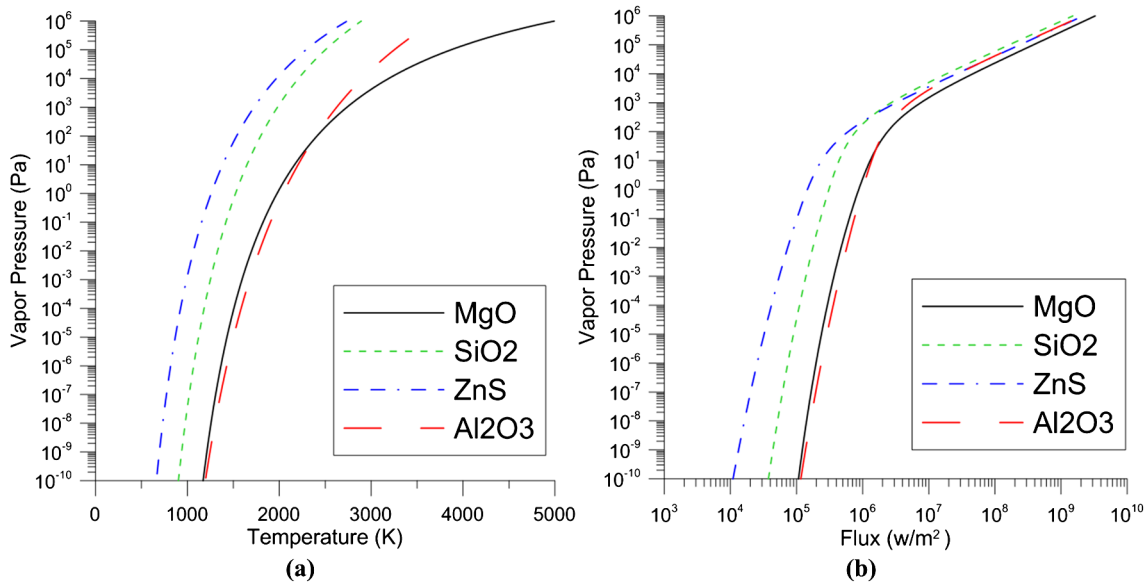
Fig. 6 (a) Vapor pressure versus *T* for four common high temperature asteroid compounds. (b) Vapor pressure versus target flux for the same found compounds. Note that at temperatures of 2000 to 3000 K or fluxes of about 10 MW/m² the vapor pressure and hence mass ejection rates are very high.

This can be seen in Figs. 5 and 6 where we model the vapor pressure in Pascals (N/m²) versus *T* and versus target flux for 93 elements. In addition, we show models for four common asteroid molecular compounds. Even vapor pressures of 10^3 Pa (0.01 atmospheres) correspond to enormous reaction forces on the asteroid and large mass ejection rates. Although we do not expect to see an asteroid of solid Tungsten we could mitigate it. Contrary to the small iron-rich meteorites that are found on the ground, a more typical asteroid looks more like the lunar surface and has quite low thermal conductivity and is thought to be a "rubble" pile in many cases, particularly for larger (>few hundred meters) asteroids. We have assumed the worst case of complete chemical binding (i.e., solid). In many cases asteroids will have significant low temperature volatile materials that may make mitigation much easier. Asteroids are also molecular rather than atomic in species in general but the conclusion are the same, namely at temperatures around 2000 to 3000 K or target fluxes of 10^6 to 10^8 W/m² all known materials will undergo vigorous evaporation. What is critical is to increase the spot flux to the point where evaporation becomes large. It is not sufficient to simply apply a large amount of total power, there has to be a large flux to initiate evaporation.

Once we understand the material properties of the targets,[5] we can design a system that is capable of evaporating them, and in this process we divert them due to the large plume thrust generated. We see in Fig. 7 at what distances we can begin to engage targets of differing compositions. For example, a comet will begin evaporation at much lower flux than a rocky asteroid, and thus we can begin to engage them at much lower total power levels and hence smaller systems or at much larger distances. These simulations assume the sun is also illuminating the targets, which accounts for the lower temperature limit. This is approximate as it is depends on the target reflectivity and orbit. The sun does not have a significant effect except in the case of comets.

2.3 Detailed Thermal Modeling

Thermal modeling is critical. We take three approaches and all yield consistent results.

The basic equations are derived from energy conservation.

Power in (laser) = Power out (radiation + mass ejection) + (dU/dt) where U = Asteroid internal energy and dU/dt is effectively from conduction. In the steady state $(dU/dt) = 0$, $P_{in} = P_{out} + (dU/dt)$, with $U = \int \rho c_v dv$, where c_v = specific heat (J/kg-K).

$$F_L = \text{LaserFlux-in} \quad \text{W/m}^2$$

$$F_{rad} = \text{Radiation Flux-out} \quad \text{W/m}^2$$

$$F_{ejecta} = \text{Ejecta Flux-out} \quad \text{W/m}^2$$

$$F_{cond} = \text{Thermal Conduction-in} \quad \text{W/m}^2$$

$$P_{in} = P_{rad} + P_{Ejecta} + P_{cond}$$

$$\oint (\bar{F}_L - \bar{F}_{rad} - \bar{F}_{Ejecta} - \bar{F}_{cond}) \cdot \hat{n} \, dA = 0$$

$$= \int \nabla \cdot (\bar{F}_L - \bar{F}_{rad} - \bar{F}_{Ejecta} - \bar{F}_{cond}) \, dv = 0.$$

Locally:

$$\bar{F}_L = \bar{F}_{rad} + \bar{F}_{Ejecta} + \bar{F}_{cond}$$

$$\bar{F}_{rad} = \sigma T^4 \cdot \hat{n}$$

$$\bar{F}_{Ejecta} = \Gamma e \hat{n} M^{1/2} (2\pi RT)^{-1/2} \alpha_e 10^{[A-B/(T+C)]} H v \hat{n}$$

$$|\bar{F}_{rad}| = \sigma T^4$$

$$|\bar{F}_{cond}| = K \nabla T$$

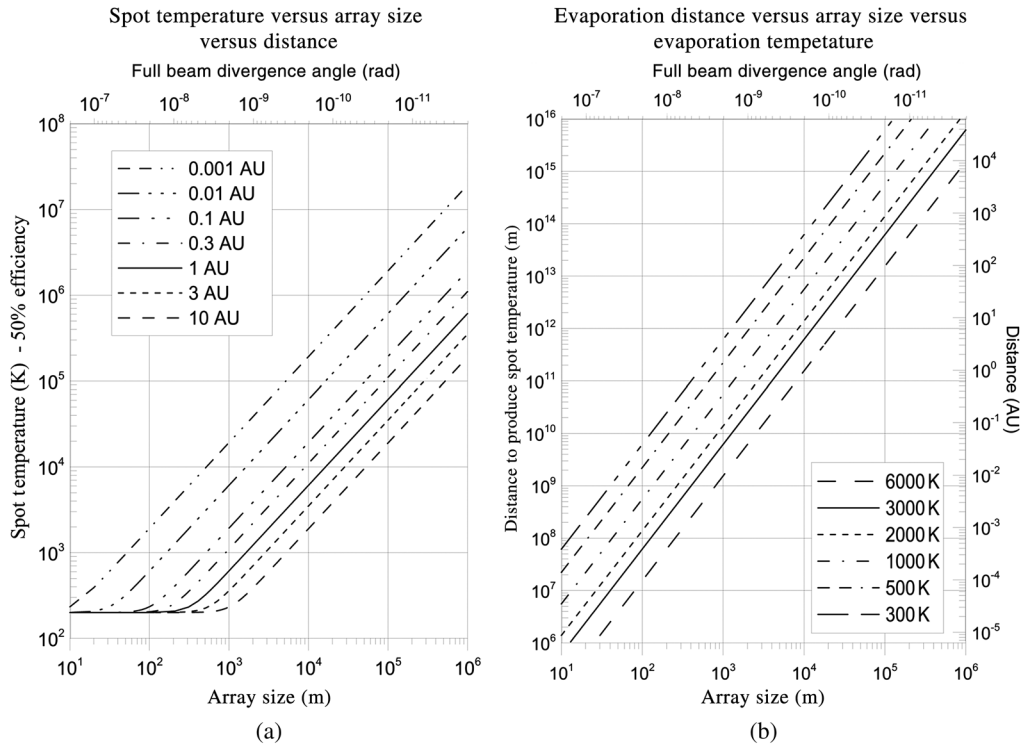$$|\bar{F}_{Ejecta}| = \Gamma e * H v,$$

Spot temperature versus array size versus distance

Evaporation distance versus array size versus evaporation tempetature

(a) (b)

Fig. 7 (a) Spot temperature versus DE-STAR array size for various target distances from 10^{-3} to 10 AU, including average solar illumination on asteroid (sets lower limit on asteroid or comet temperature). (b) Distance to target versus array size for various spot temperatures from 300 to 6000 K. At 300-K icy comets become targets while at 6000 K (hotter than sun) no known material survives.

where k is the thermal conductivity (which can be position and temperature dependent), Γe is the mass ejection flux (kg/m²-s), and Hv is the heat of vaporization (J/kg).

$$\Gamma e = \frac{M\alpha_e(P_v - P_h)}{\sqrt{2\pi MRT}} = M^{1/2}(2\pi RT)^{-1/2}\alpha_e(P_v - P_h),$$

where $M = $ molar mass (kg/mole); $P_v = $ vapor pressure (Pa); $P_h = $ ambient vapor pressure $= 0$ in vacuum; and $\alpha_e = $ coefficient of evaporation $0 \leq \alpha \leq 1$.

We model the vapor pressure for each element and compound using a semianalytic form known as Antoine coefficients.

Log $Pv = A - B/(T + C)$, where A, B, and C are unique per element and compound. These form the basis for Figs. 3 and 4.

Hence:

$$Pv = 10^{[A-B/(T+C)]}$$

$$|\bar{F}_{\text{Ejecta}}| = M^{1/2}(2\pi RT)^{-1/2}\alpha_e 10^{[A-B/(T+C)]}Hv.$$

We also assume a Gaussian profile for the laser as an approximation.

For Gaussian laser of power P_T

$$|\bar{F}_L| = \frac{P_T}{2\pi\sigma^2}e^{-r^3/2r^2},$$

where $r = $ distance from spot center. In the approximation, where the spot is small compared to the asteroid, we have:

$$\bar{F}_L = \frac{-P_T}{2\pi\sigma^2}e^{-r^3/2r^2}\hat{n}.$$

In the dynamic case, we also solve for transient heat flow by solving:

$$\nabla \cdot (K\nabla T) + \frac{d}{dT}(\rho c_v T) = 0, \quad K\nabla^2 T + \rho c_v\frac{dT}{dt} = 0.$$

In the last equation, we have assumed K (thermal conductivity) is independent of position and ρ, c_v are time independent.

In the full 3-D time-dependent solution, we use all of the above and simultaneously solve the equations using a 3-D numeric solver (COMSOL in this case).

In the 2-D steady state solutions, we assume the thermal conductivity is small (this is shown in our 3-D simulations to be a valid assumption as well as from first principle calculations) and use a combination of radiation and mass ejection (phase change):

$$|\bar{F}_L| = |\bar{F}_{\text{rad}}| + |\bar{F}_{\text{Ejecta}}| = F_T,$$

$$F_T = \sigma T^4 + M^{1/2}(2\pi RT)^{1/2}\,10^{[A-B/(T+C)]}Hv.$$

Inversion is not analytically tractable, so we use numerical inversion to get $T(F_T)$, which gives $P_v(F_T)$, $\Gamma e(F_T)$ etc.

In this inversion, we fit (to 10th order typically) $T = \sum_{n=1}^{N} a_n(\log F_T)^n$.

We use the Gaussian approximation to the laser profile (this is not critical) to get $T(r)$, $P_v(r)$, $\Gamma_e(r)$, where r is the distance from the center of the spot.

Since radiation goes as the 4th power of T while the mass ejection from evaporation goes roughly exponentially in T, at low flux levels the outward flow is completely dominated by radiation (you heat the asteroid slightly and it radiates). As the spot flux level increases (spot size shrinks or power increases or both) evaporation becomes increasingly dominant and eventually at about $T \sim 2000$ to 3000 K or fluxes of 10^6 to 10^7 W/m^2 mass ejection by evaporation becomes the dominant outward power flow and (just as water boiling on your stove) the temperature stabilizes and increasing flux increases the rate of mass ejection with only very small increases in temperature. To help understand this we plot the relationship between flux and temperature in the purely radiation dominated mode in Fig. 7.

We will briefly summarize the results from the three methods below.

- Energetics alone. Use heat of vaporization and set spot flux to $T \sim 6000$ K. No radiation or conduction included.

- 2-D—Model elements and compound vapor pressure versus T. Include radiation emission. Ignore thermal conduction.

- 3-D—Full 3-D FEA includes phase change, vapor pressure, mass ejection, radiation, and thermal conduction.

2.3.1 Energetics alone

The heat of vaporization of a compound is the energy (per mole or per kilogram) to remove it from the bulk. We can relate this to an effective speed and an effective temperature, which are related to but somewhat different than the physical speed of ejection and the physical temperature of vaporization. To be more precise, the term evaporation refers to molecules or atoms escaping from the material (for example water evaporating), while boiling is the point at which the vapor pressure equals or exceeds the ambient pressure. At any nonzero temperature there is a probability of escape from the surface, so evaporation happens at all temperatures and hence vapor pressure is a quantitative measure of the rate of evaporation. The heat of vaporization is also temperature and pressure dependent to some extent. As can be seen in Table 1, the various materials that we plot vapor pressure versus T and flux in Fig. 4 above have relatively high effective temperatures, reflecting the fact that there is a probability

distribution of energies and that the increase in vapor pressure versus T in Fig. 4 shows that the thermal probability distribution has a "tail" allowing for escape from the surface at lower temperatures that one would naively conclude from a mean analysis only. A similar analogy is the Saha equation that relates the ionization fraction versus temperature where a mean analysis would conclude that extremely high temperatures are required to ionize an atom; but, in fact significant ionization occurs at much lower temperatures due to the probability distribution tails. If we put power P_T from the laser on the asteroid in a small enough spot to heat to above the radiation dominated point [typically, 2000 to 3000 K for "rocky" asteroids (versus 300 to 500 K for comets)], we can compute the evaporation flux (mass ejection rate) as $\Gamma_e = P_T / Hv$. This is the maximum possible rate of mass ejection. We can get quite close to this maximum if we design the system properly.

2.3.2 2-D thermal calculation

As mentioned above, in this calculation, we will assume the thermal conduction is small compared to radiation and mass ejection (a good assumption for most asteroids). Using the equations above and the numerical inversions, we can solve for the temperature distribution and thus the mass ejection and thrust on the asteroid among many other parameters. We summarize some of these in Fig. 9, for example SiO$_2$. We allow σ (sigma) in the Gaussian beam profile to vary to show the effects of nonideal beam formation as well as beam and pointing jitter. The diffraction limited σ at 1 AU should be about 5 m. As can be seen, we are quite tolerant to errors in beam formation, focus, beam bitter, and pointing errors even beyond 10σ as long as the power is high enough. The requirements on a low power system at equivalent distances are more severe. We also see that we come close to achieving the theoretical maximum mass ejection rate. Also, note the thrust (N) per watt is close to 0.001 N/W. This is comparable to the Shuttle SRB in thrust per watt. This is not really surprising if you think of conventional propellants as being approximately thermal in nature with temperatures close to the maximum sustainable in the combustion chamber and exhaust nozzle (i.e., few $\times 10^3$ K).

Asteroid plume thrust. The ejecta speed from the asteroid is also close to that of a conventional rocket (few km/s). The Shuttle SRB, for reference, has a power of about 13 GW and a thrust of about 14 MN (mega newtons) and exhaust speed of around 2.6 km/s. Our computed thrust for a DE-STAR 4 with 70 GW on target is about the same (thrust) as the SRB assuming our "exhaust nozzle" on the asteroid is nearly isotropic in the forward 2π. This "plume thrust" is what is responsible for the dramatic orbital diversion that is possible with the DE-STAR system. In a power-limited system the thrust per watt is $1/v_{rel}$ where v_{rel} is the exhaust velocity. Thus a "photon rocket" or photon propelled system (one of the many other uses of the DE-STAR system is pushing a spacecraft via photon pressure) is the least efficient method (in terms of thrust/watt), but in a mass-limited system where mass is being ejected for propulsion (such as in a conventional rocket or an ion engine) the thrust to mass rate (dm/dt) is v_{rel} ($=c$ in relativistic limit) and hence photons are the most efficient (in terms of thrust/dm/dt). This is one of the basic rationales behind ion engines. They can

Table 1 List of thermophysical properties of common high temperature asteroid compounds.

Material	Hv (kJ/mole)	M (g/mole)	Hv (10^6 J/kg)	V_{eff} (km/s)	T_{eff} (10^4 K)
SiO$_2$	143	60.1	2.38	1.54	0.573
Al$_2$O$_3$	293	102	2.87	1.69	1.15
MgO	331	40.3	8.21	2.87	1.32
ZnS	320	130	2.46	1.57	1.28

Note: Here, $v_{eff} = [Hv(\text{J/kg})]^{1/2}$ and $T_{eff} = (M * Hv)/3R$, where $R = k * N_A \sim 8.31$.
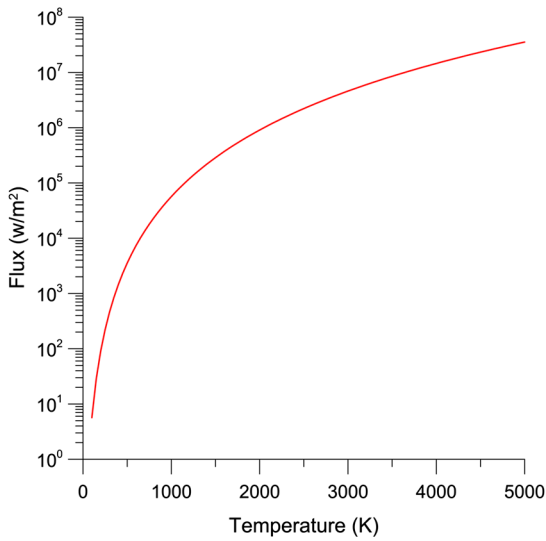
Fig. 8 Relationship between flux and temperature in spot in the radiation-dominated case. In reality the temperature rarely gets above 3000 K as power in diverted from radiation to mass ejection.

achieve much higher (nonthermal equilibrium) exhaust speeds (typically 10× or more) than a conventional propellant that is largely in thermal equilibrium. There have been proposals to use solar sails attached to asteroids as well as ion engines. Solar sails only have $F \text{ (thrust)} = 2P/c$, where P is the power intercepted from the sun on the reflector. The factor of 2 is for perfect reflection. We will use

this later for a DE-STAR standoff "photon rail gun" propulsion system.[2] The thrust per watt, in this case, is $F/P = 2/c \sim 6.6$ nN/W or more than 10^5 times lower than our plume thrust. Current state of the art ion engines (e.g., VASMIR VX-200) use 200 kW and produced 5.7 N with an exhaust speed of 50 km/s (10× shuttle main engine $H_2 - O_2$ and 20× that of the SRB which is ~2.6 km/s) and 72% efficiency using argon and a plasma exhaust equivalent $T \sim 10^6$ K with a thrust per watt of 2.85×10^{-5} N/W or about 3% of the SRB thrust/watt. This is fully consistent with the exhaust being about 20 times higher speed than the SRB and hence is should be 20 times less efficient $[5\% \times 0.72 \text{ (eff)} \sim 3.6\%]$ in terms of thrust per watt. Of course, the major advantage of an ion engine compared to a conventional propellant is that it uses much less propellant for an equivalent impulse (thrust * time), being about 20 times less and it can be throttled on and off easily. In the case of orbital modification of an asteroid, we propose using the asteroid itself as the propellant and using a high power laser driven by solar PV if attachment to the asteroid is desired. This is a modified variant of the DE-STAR system. This is a much simpler and lower mass system compared to an ion engine (which is quite massive) with extremely long life. In theory, the power required to get the same thrust as the VASMIR would be about 10 to 30 times less with this approach, but this needs to be verified in lab testing, which we are starting on.

The plots in Figs. 8 and 9 show the various parameters that come from the 2-D analysis.
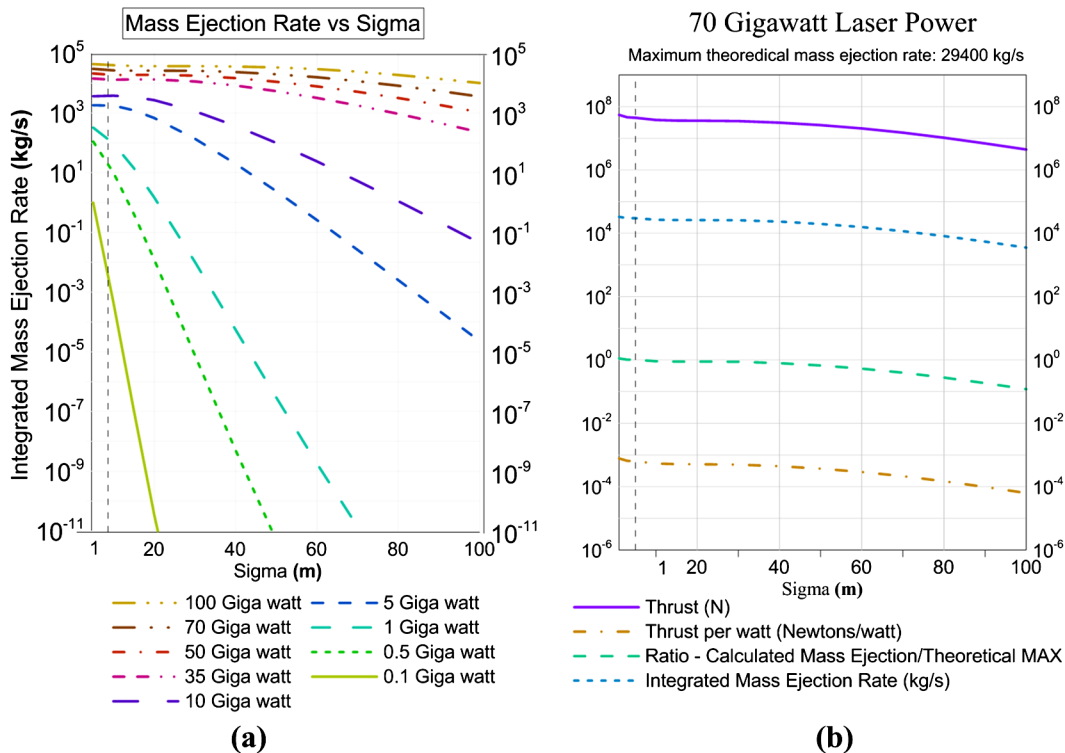

(a)

(b)

Fig. 9 (a) Mass ejection rate versus sigma (in the assumed Gaussian laser beam profile) for various power levels for the compound SiO_2. While this is done for a target at 1 AU it is independent of distance. Note that at the higher power levels, we are much more tolerant to errors that increase sigma. (b) Thrust, thrust per watt, ratio of integrated total mass ejection to maximum theoretical and integrated mass ejection versus sigma for a DE-STAR with the target at 1 AU. Nominal diffraction limited sigma is 5 m but it is clear that we have a very wide latitude (more than 10×) to absorb various errors that increase the effective sigma (beam formation, phase noise, beam jitter, and pointing jitter).
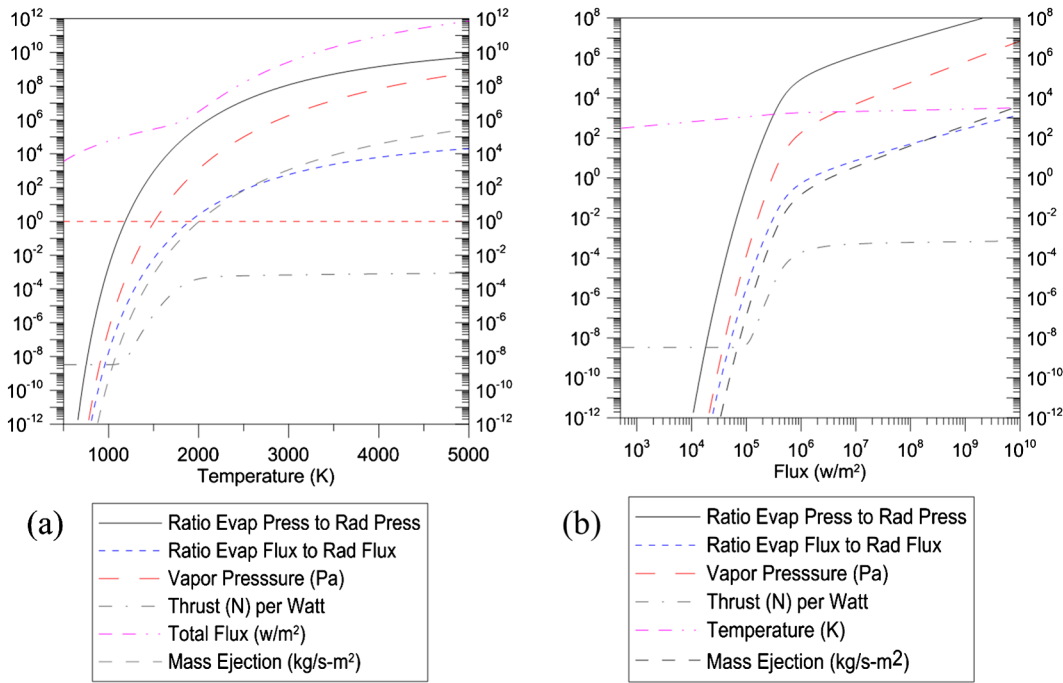
Fig. 10 (a) Simulations of SiO$_2$ properties versus temperature. (b) Simulations of SiO$_2$ properties versus flux.

Interaction simulations. In Fig. 10, we calculate various properties expected. This is done for SiO$_2$ but the results are similar for the other compounds we have simulated. The vapor pressure and mass ejection and thrust have a roughly exponential rise with temperature, but when computed versus target flux they enter a nearly linear regime above about 10^6 to 10^7 W/m^2. This is expected when the dominant flux is due to mass ejection and the vapor pressure, mass ejection rate, and thrust are all approximately linear with power above this point. This is the point above which we want our flux to be in. The surface temperature does not change much in this regime, just as a pot of boiling water remains at about 100°C at sea level independent of how high you turn up the flame. This is the same linear regime. Notice the thrust starts at the photon thrust (absorbed in this case) of about 3.3 nN/W and raises more than 5 orders of magnitude to about 1 mN/W in the linear regime mentioned above. This value then essentially remains constant at high flux, until extremely high values are reached and ionization begins.

2.3.3 *3-D thermal calculations*

In the 3-D simulations, we use all of the above as shown in the thermal transport equations, but we must numerically solve for the temperature distribution. In the model, we put radiation, mass ejection, and phase change and thermal conduction, as well as solve for both the transient and steady state case. This was done with a 3-D solver using COMSOL and modified to add mass ejection (phase change) for arbitrary materials.

Thermal conduction. Unfortunately, we cannot bring asteroids into the laboratory to study their thermal properties so we must rely on astronomical observations, primarily in the infrared, to deduce their properties combined with assumptions about their formation and likely structure. References 6–9, among many others, have done excellent work in this area, and we were able to use their results. One can derive the thermal properties by studying the time varying temperature as deduced from infrared observations. In this way the "thermal inertia I (J/m^2-K-s$^{1/2}$)" and thermal conductivity K (W/m-K) are derived. The relationship between them is: thermal Intertia (I)—(J/m^2-K-s$^{1/2}$) and thermal conductivity (K)—(W/m-K):

$$I = (\rho\,K\,C)^{1/2};\ \rho = \text{density (kg/m}^3);\ C = \text{heat capacity (J/kg-K)}.$$
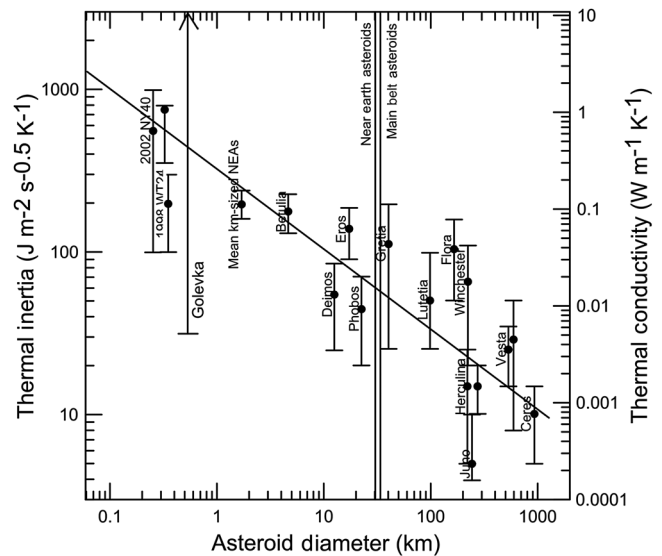

Fig. 11 Thermal properties measured for various asteroids from Delbò et al.[9]

Table 2 Common material thermal properties for comparison to the asteroid thermal properties in Fig. 8.

Material	K (W/m-K)	ρ (kg/m^3)	C (J/kg-K)	I (J/m^2-K-s$^{1/2}$)
Nickel	91	8850	448	1.9×10^4
Iron	81	7860	452	1.7×10^4
Granite	2.9	2750	890	2600
Ice (solid)	2.3	917	2000	2040
SiO$_2$ (solid)	1.04 (200 C)	2200	1000	1510
Water (liquid 0 C)	0.56	1000	4200	1500
Snow (firm)	0.46	560	2100	740
Soil (sandy)	0.27	1650	800	600
Pumice	0.15	800	900 (varies significantly)	330
Styrofoam	0.03	50	1500	47
Air	0.026	1.2	1000	5.6
Moon (regolith)	0.0029	1400	640	51

Hence:

$$K = I^2/(\rho C).$$

The graph shown in Fig. 11 is best fit to data from Delbò et al.,[9] where D is the asteroid diameter in kilometers: $I = d * D^{-\xi}$ with $d = 300$ (km) and $\xi = 0.4$; $K = 3 \times 10^4 * D^{-0.8}/(\rho C)$.

The trend (with significant errors) is toward smaller asteroids having larger thermal conductivity and larger asteroids having smaller thermal conductivity. Some of this may be the "rock pile" effect for larger asteroids. It is the values that are of interest in our models. We have assumed a relatively conservative case of $K = 1$ W/m-K.

To put this in perspective we use some values for common materials in Table 2.

Rotating asteroids. Asteroids do rotate, but generally quite slowly. We do not have a complete picture of this but from the limited data on the rotation of larger bodies and the break up speed it is estimated that asteroids in the 0.1 to 1 km class typically rotate no faster than once per hour. As is seen in our transient thermal simulations shown in Fig. 12, the mass ejection and hence thrust begins within about 1 s for a DE-STAR 4 at 1 AU. It is largely a flux issue so that for the same flux at any distance the mass ejection remains at this rate. This is assuming solid SiO$_2$, which is extremely conservative. We add loss to mimic the absorption qualities of asteroids, which are very absorptive having typical reflection coefficients around 5%. Thus, a rotating asteroid with this rate (1 h) poses little problem. Similar issues are encountered by efforts to de-orbit space debris.[10] More interesting perhaps is can we spin up (or down) an asteroid depending on beam placement?

3-D results. We have run hundreds of 3-D models and will show a few salient results, as in Fig. 12. Perhaps the most interesting bottom line is that the simplest assumptions we started with, namely energetics only and conservation spot flux, were borne out as being valid but we now have much more sophisticated tools with which to analyze and optimize the system.

Comparison of 2-D and 3-D simulations. While the 3-D simulations give us time-transient solutions and include full thermal conduction, they lack the numerical flexibility of the
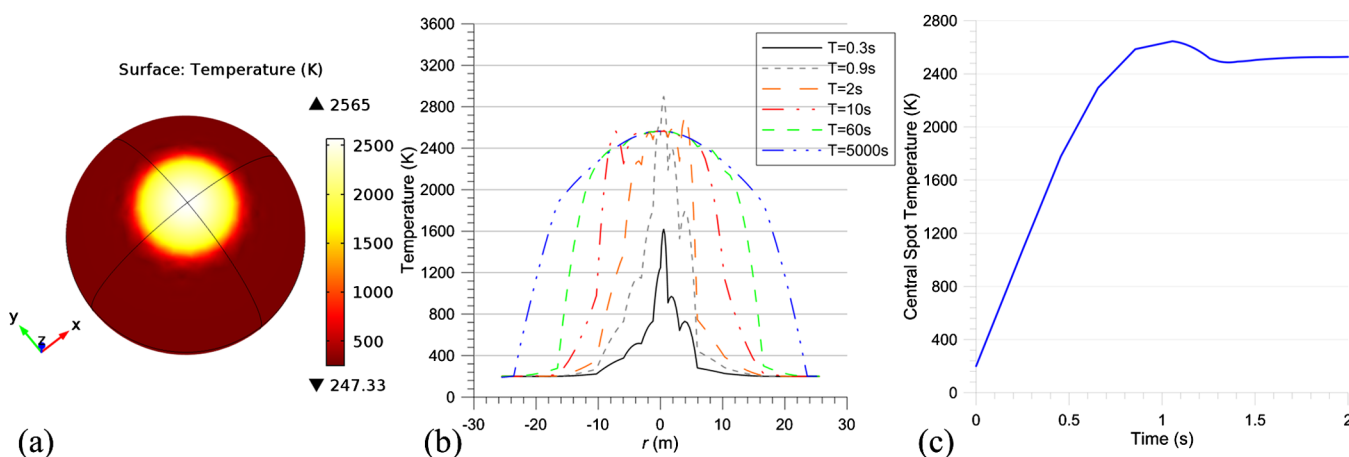

Fig. 12 All cases refer to SiO$_2$ as the equivalent material. (a) Steady state surface temperature distribution for a 100-m diameter asteroid at 1 AU with a DE-STAR 4 Gaussian beam de-rated to 50 GW. Spot diameter is ~30 m. Temperatures rise to the point of being mass ejection limited, which is about 2600 K in the center of the spot. Solar illumination with an isotropic average of 350 W/m^2. (b) Temperature distribution versus theta (angle from beam axis). High frequency substructure is due to numerical meshing. (c) Transient time solution of temperature in the spot center (K) versus time (s) after the laser is turned on at $t = 0$. Initial temperature is 200 K. Mass ejection begins within 1 s.
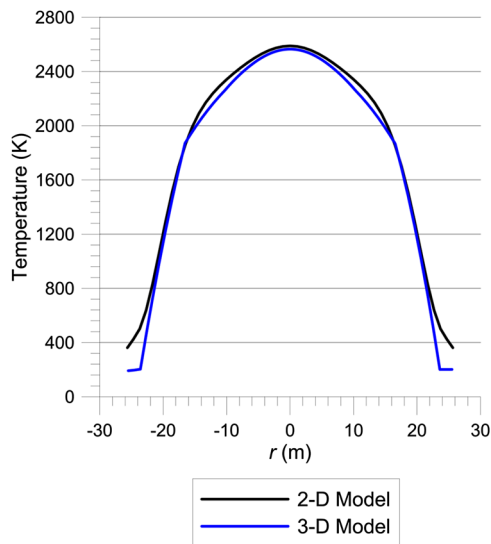
Fig. 13 Comparison of 2-D and 3-D models temperature versus theta (angle from beam axis on sphere) for SiO_2 with 50-GW total power and sigma $= 5$ m Gaussian beam illumination. Results are nearly identical in the critical central region.

2-D solutions. We compared the results of the temperature distributions for a Gaussian laser illumination and found them to be very close in their predictions. This gives us confidence that we can do both 2-D and 3-D simulations with high fidelity. The ultimate test will come when we compare the laboratory tests that we are currently executing. In Fig. 13, we compare the temperature distribution for a 3-D model (blue) with a 2-D model (black). They have nearly identical results in the critical center of the spot and then differ in the wings. This is close enough for our needs now. As we refine the laboratory tests, we will feed the results back into the models.

2.4 Orbital Diversion via Plume Thrust

In general, we do not need to evaporate the asteroid to avoid an impact scenario. It is sufficient to change its orbit enough to miss the earth. The ability to standoff and divert using the plume thrust that DE-STAR generates is an extremely attractive approach. Consider the example of Apophis. It is approximately 325 m in diameter with a mass of 4×10^{10} kg and has an orbital speed of 30.7 km/s with a 30-h rotation. A direct hit would have a yield approaching 1 GT (Gigaton TNT). This would be a bad day. The momentum is approximately $p = mv \sim 1.2 \times 10^{15}$ N-s. If we could achieve our theoretical thrust-to-power ratio of 1 mN/W then the thrust with a DE-STAR 4 would be 7×10^7 N. If we were to activate DE-STAR for 1 month we would achieve a change in momentum of Apophis of $\delta p \sim 1.7 \times 10^{14}$ N-s. The effect on the orbit depends on the details of when and where we begin the interaction, but we can estimate the deflection angle to be $\delta\theta \sim \delta v/v = \delta p/p \sim 0.14$ radians or a $\delta v \sim 0.14 v \sim 4.2$ km/s. This is enormous by standards the deflection community speaks of. A simplistic distance deflection is given by δr (miss distance) $\sim L\delta\theta$ ($L = 1$ AU 1.5×10^{11} m) $\sim 2 \times 10^{10}$ m $\sim 3000 \times$ Earth radii. This is 50 times the Earth–moon distance. This is obviously extremely conservative and we can back way off if needed.

2.5 Laboratory Testing

A test system was constructed to check our calculations and simulations. This work is still ongoing but we show some of the results. The laser consisted of 19 fiber CW lasers, each of which was homogenized in a 800-μm core fiber and then reimaged to simulate active phase control. Each fiber had a diameter of about 150 μm and was fed with 2.1-W diode laser at 808 nm. The beam diverge with a NA $\sim$ 0.2 and reconverge with a roughly 1:1 ratio to produce a spot that was about 1 mm in diameter. Fluxes up to 40 MW/m^2 (40 watts in a 1-mm spot) are achieved, which is close to the target of a DE-STAR 4 at 1 AU; see Fig. 3. For reference the surface of the sun (assuming a 5800-K surface) has a flux of about 60 MW/m^2. When we fire the laser at a target, we do indeed create an extremely intense white hot spot that lights up the room and vaporizes every material we have tried. So far our tests are done outside the vacuum chamber but vacuum tests will begin shortly. Diagnostics include IR (out to 12 μm) and visible light cameras as well as a fiber fed optical spectrometer. Optical coupling from fiber tip to target was measured at about 90%. Mass ejection was definitely observed (holes were punched through) but quantitative comparison to a mass ejection model will be done in vacuum as the vapor pressure would have to exceed 1 atm for normal evaporation. For basalt, the measured (in 1 atm air) was 0.42 mg/s while the theoretical maximum for this test was 2.2 mg/s. One significant issue is the complex nature of the test materials we are evaporating. We will use some standard targets in the vacuum tests. Air convection is also a serious issue, so it is not surprising that our mass ejection is less than anticipated for a variety of reasons. We did try plain sand from the local beach and placed it in a small crucible and melted it into a glass ball, as well as vaporized some of it. Figures 14 and 15 depict setup of vaporization experiments and initial comparison to model results.

2.6 Ground versus Airborne versus Space-Based Systems

While the baseline for DE-STAR is an orbital approach, a ground-based approach offers many obvious advantages in terms of testing and deployment, while the severe impediment of the atmospheric perturbations may be insurmountable for the foreseeable future. In all of our initial "roadmaps" to DE planetary defense, ground deployment for the smaller systems during test and debugging is a crucial step. The great strides made in adaptive optics for astronomy and situational awareness allow sub-arc-second beam formation. Based on the active laser guide star programs microradian beam formation is feasible from the ground. The transmission on clear days from excellent ground-based sites allows for <10% transmission loss near 1 μm from ground to space. On cloudy days, the transmission will be essentially zero. However, it is not the transmission which is the critical issue. It is the atmospheric turbulence or "seeing"—phase perturbations in the beam formation that is the limiting factor. One great advantage of a phased array approach is that every aperture element is part of an "adaptive optics system" by the very nature of the phased array. In addition, rather than mechanically adjusting the phase front across a sub optic in a classical adaptive optic system, the DE-STAR will have much higher servo phase control bandwidth. This will lead to greatly improved adaptive optics
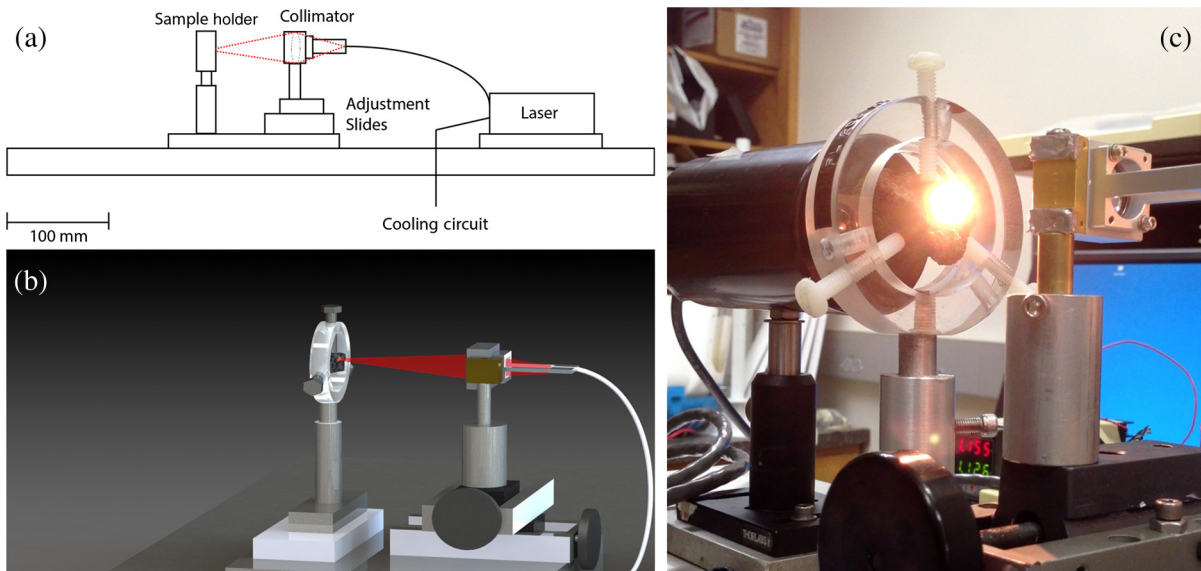
Fig. 14 (a) Cross section diagram showing laser (which is 19 individual fiber fed lasers) and the recollimating optics. (b) Rendering showing beam expansion and imaging as well as sample holder. (c) Laser firing at a target (basalt in this case).
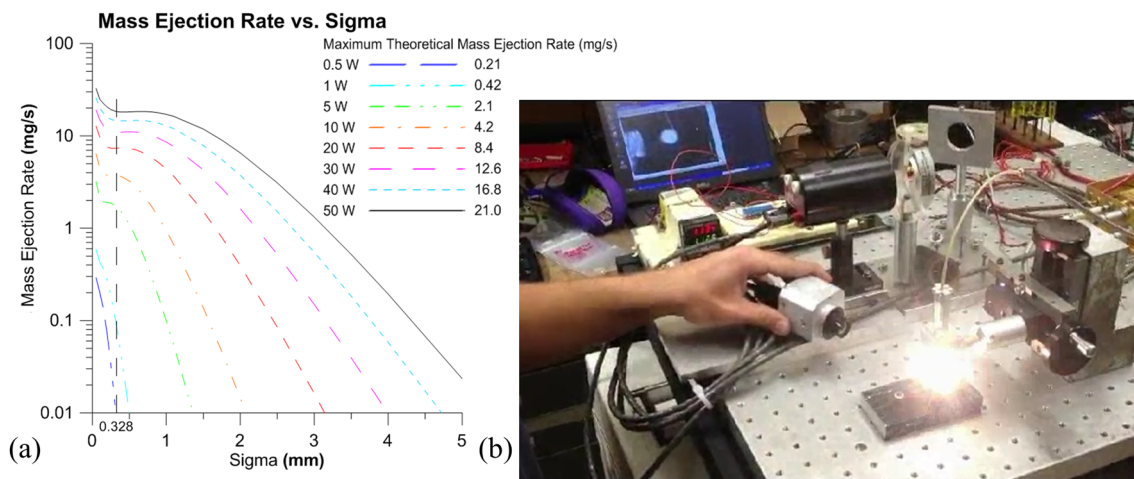

Fig. 15 (a) 2-D simulation with laboratory test parameters. Similar to Fig. 7 but set for lab testing. Plot is of expected mass ejection versus sigma (Gaussian beam) for various power levels. Measured sigma based on whole size in targets is <330 μm. Sample is assumed to be SiO_2. (b) Picture of test system. Small camera is a 8 to 12 μm FLIR IR microbolometer unit. Sample is sand in this video. The sand was melted and vaporized. (Video 1, MOV, 2.66 MB) [URL: http://dx.doi.org/10.1117/1.OE.53.2.025103.1, or http://www.deepspace.ucsb.edu/projects/directed-energy-planetary-defense].

performance, the limits of which are still to be explored. The early and smaller versions of DE-STAR, such as a DE-STAR 1 (10-m aperture) can be used from the ground to explore not only system design and performance but also may allow for initial space debris mitigation. As can be seen from Fig. 3, the beam size θ (nrad) for an aperture size d(m) system is $\theta(\text{nrad}) \sim 2 \times 10^3/d$. For reference, the "seeing" from an excellent ground-based mountain top site (e.g., Mauna Kea) is about 2-μrad RMS at 1-μ wavelength. Ground-based seeing is typically given in arcseconds, where 1 arcsec $\sim$5 μrad, while adaptive optics are often quotes in wavefront error (often in nanometers) or in milliarcsec (mas) where 1 mas $\sim$5 nrad. It is important to note that seeing is usually much more stable at night due to thermally driven perturbations

during the day and that the "seeing" quoted for ground-based systems is for night time operation. With adaptive optics and decent Strehl ratios ($\sim > 0.5$), 50 mas or 250 nrad at 1-μm wavelength is expected when using multiple active laser guide stars being planned for the next generation of extremely large telescopes such as the thirty meter telescope among others when operated at night (of course). This (250 nrad) is approximately the beam size for a DE-STAR 1. Extremely aggressive sites, such as being above the boundary layer at Dome A, may allow even better adaptive optics and would be a possibility for small DE-STAR deployments. The extremely high-speed phase control of DE-STAR may allow even better Strehl ratios. This territory needs to be explored. For systems capable of true planetary

defense (DE-STAR 3 or 4) one would need have 100 to 1000 times smaller beams and thus ground-based deployment. While not impossible to imagine someday, is not likely to be effective with currently understood technologies for atmospheric perturbation mitigation. However, this area should be explored. In order to perform a proper analysis the issues of weather (cloud cover, etc.) and day/night seeing would have to be factored in. Daytime adaptive optics is also a complicated issue that needs further study.

Airborne platforms offer the advantages of reduced atmosphere but usually severe operational constraints. Fixed-wing aircraft are particularly problematic due to high-speed turbulence and airframe microphonics. Airship and balloon-borne platforms are another alternative as balloons operate at above 30 km with near zero relative airspeed. Balloon-borne platforms are viable for the smaller DE-STAR systems for multiple uses but one of the primary issues is power. Beamed power from the ground is one option that we have studied in some detail for other programs. One could imagine large fleets of airship or balloon-borne platforms, but it does not seem feasible for all but the smallest systems.

Space-based deployment offers many advantages with the severe disadvantage of launch cost. Much of our current focus is on ultralow areal mass systems with a goal of under 1 kg/m² for overall areal density. With the exception of thin-film holographic lenses, no current technology can meet this goal. We are actively working on this optical possibility. The lowest launch energy solution is an low-earth orbit (LEO) sun synchronous orbit to allow constant (except for eclipses) solar illumination and a relatively constant thermal environment. More stable orbital environments such as at a Lagrange point or possibly at geosynchronous orbits are more costly to achieve and vastly more complex to service. A lunar surface deployment might be another choice but again is much more difficult logistically and much more costly to deploy but could be a future defensive position for the Earth.

2.7 Pointing Issues

The pointing requirements of the DE-STAR system are one of the more difficult technical challenges. Ultimately, the requirements for achieving high flux on target drives the overall pointing and thus the sensing and servo feedback loops. Unlike a classic optical system, a phased array offers both advantages and challenges compared to the bulk rigid body requirements of a system like the HST. The subelement sizes of even the largest DE-STAR units are currently baselined to be in the meter diameter class (shroud-size limited). We can learn from the experience with rigid body pointing from the HST and upcoming James Webb Space Telescope (JWST), as well as many other space-based telescopes. As mentioned, the HST had a 24-h RMS of 35 nrad. If we imagine each subelement being pointed to this level but with uncorrelated pointing errors to its neighbors (clearly there will be some crosstalk) the question is "what will the overall affect be on the synthesized beam?" We are simulating this now and this will be covered in a future optical design paper. Since the beam from a 1-m subelement (as an example) has a beam size of ~2 μrad, the individual element pointing error can be much smaller than the individual element beam size. Correlated pointing errors are a much more serious issue and one where the overall feedback loop needs to feed

information to correct for the final beam pointing. This is a nontrivial problem and one where significant work needs to take place for the largest systems where subnanoradian final beams need to be synthesized.

We have simulated a related effect of phase errors extensively. Here, the effect is opposite of the effect of pointing errors. For phase errors, complete correlation of the phase errors (or overall shifts) is cancelled out to first order since it is the phase differences and not the absolute phase that is important. Large-scale correlated phase errors are important, however. For example, a linear phase shift across the array would be equivalent to a pointing error. Again, the servo loop must correct and control the phasing to make a phased array.

We have simulated the effects of random phase error as might arise from phase noise in the amplifiers or high frequency (beyond the servo bandwidth) mechanical vibrations. We have run a Monte-Carlo simulation with RMS phase errors of 10^{-3} to 1 wave (2π equivalent phase) and from 2 to 10^4 elements of individual sizes from 0.01 m to beyond 1 m and find that our initial assumption of maintaining 1/10 wavefront error is a reasonable one, though 1/20 would be significantly better. Results are shown in Fig. 16. We have compared our simulations to simple Ruze theory (which is technically not appropriate due to the assumptions of correlation sizes in Ruze theory). We use the relationship[11]

$$\frac{\langle I \rangle}{I_o} = \frac{1 - e^{-\sigma_o^2}}{N} + e^{-\sigma_o^2},$$

where I_0 is the flux with no phase perturbation, $\langle I \rangle$ is the expected value of flux with phase perturbations, σ_0 is the
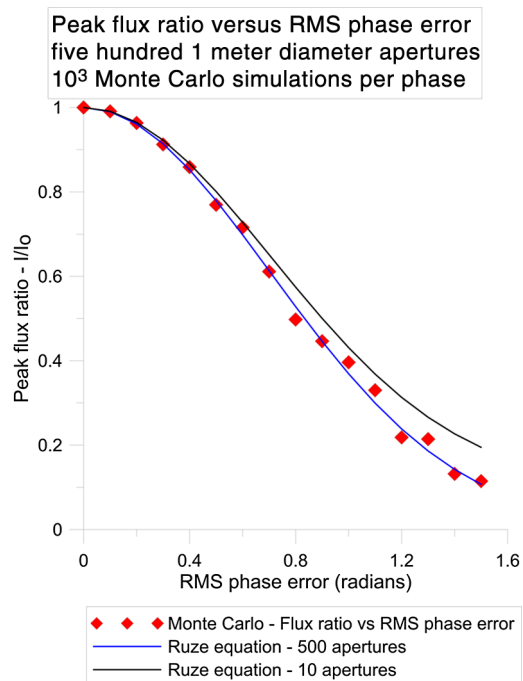

Fig. 16 Results of Monte-Carlo simulations compared to the Ruze relationship between phase error and peak flux ratio. As more phase error is present, power leaks from the central lobe and is dispersed into side lobes.

RMS phase perturbation with zero-mean Gaussian distribution, and N is the number of elements. We find our simulations agree extremely well with the simple Ruze exponential roll of forward gain or flux on target where in the limit of infinite number of aperture becomes $I = I_0 \, e^{-Var(\phi)}$ where $Var(\phi)$ is the variance of the phase per element, I is the flux on target with phase perturbations, and I_0 is the flux on target with no phase perturbations.

2.8 Asteroid Rotation Surveys

As briefly discussed above, asteroids do rotate since there is always some angular momentum they acquire in formation. There have been a number of studies of asteroid rotation with data primarily from the reflected light curves.[12] Although there is no complete survey of small (say >30 m) distant asteroids (1 AU for example) due to the difficulty in detecting them, we can draw general conclusions from the several thousand that have been measured. Larger asteroids tend to be loosely bound and essentially that of a "rubble pile"—namely a collection of material that is on the large level gravitationally bound and on the smaller level molecularly bound. The transition between the gravitational binding and molecular binding seems to occur in general around 100 m in diameter with some significant exceptions at smaller diameters where gravitational binding can dominate. It is easy to prove that for a constant density rotating sphere that is gravitational bound the critical rotation period is $\tau_{\text{crit}}(s) = (3\pi/G\rho)^{1/2} \sim 1.2 \times 10^4 \rho^{-1/2}$ (g/cc) with periods shorter than this being unstable and unbound and longer periods being stable "rubble piles." This is independent of the diameter of the asteroid. For a density of typical asteroid rubble of $\rho \sim 2$ g/cc this gives $\tau_{\text{crit}} \sim 2.3$ h. When looking at the measured light curves, which reflect (literally) the rotation period of the asteroid, one sees a remarkably sharp cutoff at very close to 2.3-h consistent with asteroids larger than about 200 m in diameter being gravitational-bound rubble piles. The worst case is an asteroid approaching with spin axis perpendicular to the line of sight. The critical comparison is then the surface speed compared to the beam size and the heating time to produce mass ejection. In Fig. 12, we showed the rapid rise to mass ejection for the DE-STAR 4 system with a 1 AU rocky target started in ~1 s after illumination. A 200-m diameter asteroid rotating with a 2.3-h period has a worst case surface rotation speed of about 0.08 m/s compared to a 30-m diameter spot size and thus the spot dwell time is $\sim 30/0.08 \sim 400$ s or much longer than the time to mass ejection (about 1 s). Even kilometer-class asteroids rotating with the same period would not rotate too fast for mass ejection to begin. At the extremely fast end of rotation there are a few known 100-m diameter class asteroids (not rubble piles) that appear to rotate with periods as short as 1 min (this is truly exceptional) and in this case the worst case surface speed would be 9 m/s or a spot dwell time of 3 s. Even in this extreme case the beam would begin ejection. At smaller diameters there may be a tightly bound rapidly rotating asteroid (Fe/Ni for example) that may pose a problem. These are less hazardous in terms of impact energy, and we are looking at absolutely worst case rotations (of which none are known), but even in this case as the asteroid gets closer to Earth the flux rises as the spot shrinks and the mass ejection happens faster. These do not appear that they would survive being illuminated as they have less mass and momentum to start with. An interesting question in case asymmetric illumination causes spin up or spin down of a rotating asteroid. Could this be used to cause disruption from plume "spin up" or be used to slow down an asteroid for capture? A related issue is that of rotating space debris, as discussed in Ref. 10.

2.9 "Stand-on" Applications—DE-STARLITE

Although the primary motivation for DE-STAR has been as a "standoff defense" system it can be used in a variety of modes where much smaller systems can be used as "stand-on" systems. The use of the same system in miniature to get close to a target and then use the focused laser in the same mode but at much closer distances allows for applications where a high flux laser can be used for remote laser machine of targets in asteroids, or even lunar or Martian mining, as well as for asteroid deflection via the same "plume thrust" mechanism we have outlined above. An example of this is the DE-STARLITE mission where a small (1 to 100 kw) system is taken near to the asteroid and mass ejection is initiated. The advantage compared to a simple mirror focusing on the asteroid is that the mirror must have an $F\# < 3$ to be effective on high-temperature rocky compounds, which requires getting the mirror extremely close to the asteroid (typically 10 to 100 m away). The reason the $F\#$ has to be so low, for a mirror, is that the sun is not a point source and the flux on target is the flux at the surface of the sun/$F\#^2$. The flux at the surface of the sun is about $60 \, \text{MW/m}^2$ and thus with an $F\# = 2$ mirror the spot flux on the target would be about $4 \, \text{MW/m}^2$ which is just barely enough to start significant evaporation of rocky materials. An $F\# = 1$ mirror would be much preferred in this case. This is the same reason a simple mirror at the Earth will not evaporate distant asteroids unless the mirror diameter is roughly the size of the distance to the target (i.e., 1-AU mirror diameter!). Although using mirrors close to an asteroid is not insurmountable, the close proximity can cause severe optical pitting and dust buildup on the mirror. DE-STARLITE can standoff some 1 to 100 km away from the target and does not require sun-target alignment allowing much more flexible steering. The DE-STARLITE can also run pulsed if needed for more flexible mission scenarios. In all of these cases, the asteroid material is converted into its own propellant offering a much more efficient and powerful thruster than an ion engine of equivalent power and needs no propellant other than the asteroid itself.

3 Other Uses for DE-STAR

3.1 Summary of Other Uses

The DE-STAR is a standoff directed energy system and there are a number of other uses that are possible. We have explored some in detail and are exploring others. Clearly, if you can "laser machine" on solar system scales this brings up some thought provoking discussions.

Some of the more mundane ideas are:

- Space debris mitigation—a small unit (DE-STAR 1) is extremely effective against space debris. A unit attached to the ISS would be very useful in clearing out orbital debris.

- A LIDAR mode for refining the orbital parameters of asteroid. DE-STAR is extremely bright and makes an excellent "flashlight" to target asteroids with in order to detect and refine their positions. As an aid to existing efforts is can be quite useful. The narrow bandwidth allows for extremely low background searches as well as Doppler velocity determination.

- Standoff composition analysis—the bright heated spot might be used as a backlight to determine asteroid ejecta composition. We have begun an analysis of this to see what is feasible.

- Orbital capture—modifying the orbits of asteroids may allow for easier capture if desired.

- Beam power to distant probes—the system can be used to beam power to very distant spacecraft. At 1 AU the flux is 70 MW/m^2 or about 50,000 times the flux of the sun. At the edge of the solar system (30 AU) it is about 80 kW/m^2. At 225 AU the beam is about as bright as the sun is above Earth's atmosphere. Similarly, it could be used to provide power to distant outposts on Mars or the Moon or literally to machine on the lunar surface (or possibly Mars). The latter would be a complex sociological and geopolitical discussion no doubt.

- Spacecraft rail gun mode—while photon pressure is modest, it is constant until the beam diverges to be larger than the reflector. In a companion paper, Bible et al.[2] discuss using this mode to propel spacecraft at mildly relativistic speeds. For example, a 100-, 1000-, 10,000-kg spacecraft with a 30-m diameter (9 kg, 10-μm-thick multilayer dielectric) reflector will reach 1 AU (~Mars) in 3, 10, 30 days. Stopping is an issue! The 100-kg craft will be going at 0.4%c at a 1 AU and 0.6%c at the edge of the solar system. This is 1800 km/s at the edge of the solar system with just a 30-m reflector. This speed is far greater than the galactic escape speed and nearly 100 times faster than the Voyager spacecraft. If a reflector could be built to intercept the beam out to the edge of the solar system (900-m diameter) the same craft would be going 2% at the edge of the solar system and 3% if illumination stayed on for about 2 months. We do not currently know how to build kilometer-class reflectors that are low enough mass, though we do know how to build 30-m reflectors and 100 m appears feasible. There is work on graphene sheets that may allow for future extremely large, extremely low mass reflectors that may allow for fully relativistic speeds. Future generation may build even larger DE-STAR 5 and 6 units to allow highly relativistic probes.

- Laser driven launch and boosters—a high-power ground-based DE-STAR could be used for launch purposes when used as an ablation[13] or plume thrust driver. Similarly, for orbital boost from LEO to GEO and beyond, a DE-STAR could be extremely useful.

- SPS mode—beam power to the ground via microwave or millimeter wave. The system would produce about 100 GWe. U.S. consumption is about 440-GWe average (1400 W/person-ave).

- Interstellar beacon—we appear brighter than the brightest nighttime star at 1,000ly (typ distance to Kepler discovered exoplanets). Optical SEI use is being explored for both transmit and receive modes.

- Ultra high-speed IR communications—the calculated data rates for DE-STAR to long range, even interstellar probes is enormous with megabits per second speeds back to Earth from probes at the nearest stars for relatively small spacecraft transmitters and reflectors.

4 Conclusions

The DE-STAR system represents a solution to asteroids and comets that threaten the Earth. The same system can be used for a multitude of other purposes and thus is not a single-use system waiting for an asteroid. Its use in spacecraft propulsion, space debris mitigation, and SPS use could more than justify its cost let alone its ability to protect the Earth from catastrophe. Being modular and scalable, the DE-STAR can be built in stages as technology progresses. Small DE-STAR 0 (1 m) and DE-STAR 1 (10 m) class units can be built, tested, and even flown on suborbital platforms to test the basic concepts as small orbital versions are built. The technology is improving rapidly and is already nearly "there" in terms of conversion efficiency. There are many other uses that we have not touched on here for brevity. We propose a logical progression from the smaller DE-STAR ground and suborbital units to small orbital units as the technology improves and laser mass power density improves, until we can deploy a full-scale system such as a DE-STAR 4. As humanity becomes more technologically advanced, even larger systems can be envisioned, including systems that will allow the first interstellar probes.

References

1. G. B. Hughes et al., "DE-STAR: phased array laser technology for planetary defense and other scientific purposes," *Proc. SPIE* **8876**, 88760J (2013).
2. J. Bible et al., "Relativistic propulsion using directed energy," *Proc. SPIE* **8876**, 887605 (2013).
3. M. A. Vorontsov et al., "Adaptive array of phase-locked fiber collimators: analysis and experimental demonstration," *IEEE J. Sel. Top. Quantum Electron.* **15**, 269–280 (2009).
4. T. Y. Fan, "Laser beam combining for high-power, high-radiance sources," *IEEE J. Sel. Top. Quantum Electron.* **11**, 567–577 (2005).
5. R. P. Binzel et al., "Spectral properties and composition of potentially hazardous asteroid (99942) apophis," *Icarus* **200**, 480–485 (2009).
6. M. Mueller, "Surface properties of asteroids from mid-infrared observations and thermophysical modeling," (2007).
7. M. Mueller, A. W. Harris, and A. Fitzsimmons, "Size, albedo, and taxonomic type of potential spacecraft target Asteroid (10302) 1989 ML," *Icarus* **187**(2), 611–615 (2007).
8. A. W. Harris, "A thermal model for near-earth asteroids," *Icarus* **131**, 291–301 (1998).
9. M. Delbò, A. Cellino, and E. F. Tedesco, "Albedo and size determination of potentially hazardous asteroids: (99942) apophis," *Icarus* **188**, 266–270 (2007).
10. D. A. Liedahl et al., "Pulsed laser interactions with space debris: target shape effects," http://arxiv.org/abs/1305.3659 [physics.space-ph] (2013).
11. L. R. D'Addario, "Combining loss of a transmitting array due to phase errors," IPN Progress Report 42–175 (2008).
12. B. D. Warner, A. W. Harris, and P. Pravec, "The asteroid lightcurve database," *Icarus* **202**, 134–146 (2009).
13. J. W. Campbell et al., "The impact imperative: laser ablation for deflecting asteroids, meteoroids, and comets from impacting the earth," *AIP Conf. Proc.* **664**, 509–520 (2003).

Philip Lubin is a professor of physics at UC Santa Barbara. He received his PhD in physics from UC Berkeley. His primary work is in studies of the early universe, and he is corecipient of the Gruber Prize for Cosmology in 2006. He has more than three decades of experience in designing, building, and deploying far IR and millimeter wave system for ground, airborne, and orbital applications.

Gary B. Hughes is an assistant professor in the Statistics Department at California Polytechnic State University in San Luis Obispo, California. He received his PhD in earth and environmental science from the University of Pennsylvania.

Johanna Bible is a student in the College of Creative Studies and the UC Santa Barbara physics department.

Jesse Bublitz is a student in the College of Creative Studies and the UC Santa Barbara physics department.

Josh Arriola is a student in the UC Santa Barbara chemistry department.

Caio Motta is a student in the UC Santa Barbara physics department.

Jon Suen is a PhD student in the UC Santa Barbara department of electrical and computer engineering and with expertise in far IR and Terahertz systems.

Isabella Johansson is a student in the physics department at Santa Barbara City College.

Jordan Riley is a student in the UC Santa Barbara physics department.

Nilou Sarvian is a student in the UC Santa Barbara Chemistry department.

Deborah Clayton-Warwick is a student in the UC Santa Barbara physics department.

Jane Wu is a part of the research mentorship program at UC Santa Barbara in the physics department.

Andrew Milich is a part of the research mentorship program at UC Santa Barbara in the physics department.

Mitch Oleson is a part of the research mentorship program at UC Santa Barbara in the physics department.

Mark Pryor is president and CEO of Vorticy Inc., a San Diego-based company specializing in composite material design and fabrication for space-based applications among other uses and is formerly with composite optics and ATK. He has a master's degree from UC Santa Barbara in mechanical engineering.

Peter Krogen is a PhD student at MIT in electrical engineering working on laser electro-optics.

Miikka Kangas has a PhD in physics from UC Santa Barbara and has more than a decade of expertise in infrared systems and mm wave systems.

Hugh O'Neill has a PhD in physics from UC Santa Barbara, specializing in millimeter-wave studies of the early universe, and is currently a lecturer at California Polytechnic State University in San Luis Obispo, California.